

## Rewrite Characteristics of a Scattered-Type Superresolution Near-Field Structure Optical Disk with a Ag<sub>2</sub>O Mask Layer

Hiroo UKITA and Naoyoshi TAMURA

Faculty of Science and Engineering, Ritsumeikan University, 1-1-1 Nojihigashi, Kusatsu, Shiga 525-8577, Japan

(Received April 20, 2007; accepted May 30, 2007; published online September 7, 2007)

On the basis of the working mechanism of a silver-oxide-type superresolution near-field structure (super-RENS) disk, we realized excellent rewriting by performing the following steps: (1) initialize the disk at a continuous power of  $P_i = 8.0$  mW for 3 s, (2) write at a pulsed power of  $P_w = 8.0$ – $9.0$  mW, (3) read (reinitialize only the mask layer) at a superresolution power of  $P_{sr} = 5.5$  mW, which lies between the powers under reversible conditions of  $P_i^l = 4.5$  mW and  $P_i^u = 6.0$  mW for the mask layer, (4) erase at a continuous power of  $P_e = 7.5$  mW for 3 s, and (4) rewrite at a pulsed power of  $P_w = 8.0$ – $9.0$  mW. The carrier-to-noise ratio (CNR) difference between writing and erasing slightly varies for successive rewritings, resulting in CNR = 23 dB after 20 rewrite operations for a mark length of 400 nm, which is less than the resolution limit  $\lambda/4NA = 413$  nm. The Ag<sub>2</sub>O mask layer is decomposed into Ag nanoparticles at 160 °C that aggregate to form nanoclusters dispersed in the mask layer after the initialization operation at  $P_i = 8.0$  mW (3 s), and the recording layer made of Ge<sub>2</sub>Sb<sub>2</sub>Te<sub>5</sub> (GST) is transformed by a second phase transition from a rocksalt crystal structure of fcc to a hexagonal crystal structure (the phase transition temperature range is estimated to be 250–450 °C) at a pulsed power of  $P_w = 8.0$ – $9.0$  mW, and *vice versa* at a continuous power of  $P_e = 7.5$  mW for a disk velocity of 2 m/s. [DOI: 10.1143/JJAP.46.5838]

KEYWORDS: rewritable, superresolution, super-RENS, Ag<sub>2</sub>O, GeSbTe, second phase transition

### 1. Introduction

A scattered-type superresolution near-field structure (super-RENS) optical disk with a silver oxide (AgO<sub>x</sub>) mask layer<sup>1–3</sup> has been proposed to significantly improve the carrier-to-noise ratio (CNR) of an aperture-type super-RENS. The Ag nanoparticles in the gas bubble pit formed in writing enhance the near field (surface plasmons on the particles). Ho *et al.* found that the functional structure<sup>3</sup> of AgO<sub>x</sub> depends on write power; an aggregated Ag nanocluster (which exhibits high reflectivity due to Ag particles) efficiently scatters the near field, and the Ag ring (which exhibits high transmissivity due to a nanoaperture) not only confines the input laser beam so that it is thin, but also enhances the scattering field. Ukita *et al.* presented a read/write mechanism of a super-RENS optical disk with the structure of PC substrate (0.6 mm)/ZnSiO<sub>2</sub> (170 nm)/AgO<sub>x</sub> (15 nm)/ZnSiO<sub>2</sub> (15 nm)/GST (15 nm)/ZnSiO<sub>2</sub> (20 nm), along with results obtained from systematic experiments under various read/write conditions.<sup>4</sup>

Kataja *et al.* numerically studied AgO<sub>x</sub>-type super-RENS phenomena using a two-dimensional (2D) finite difference time domain (FDTD) method.<sup>5</sup> They indicated that an AgO<sub>x</sub>-type super-RENS can be produced beyond the resolution limit when the aperture is surrounded by Ag nanoparticles.

Nevertheless, rewriting performance has not been reported yet. In this paper, we, for the first time, find and propose a rewrite method involving the control of the phase of the mask and that of the recording layers independently by initializing the mask at superresolution read power or at erase power.

### 2. Read/Write Mechanism of a Scattered-Type Super-RENS with a AgO<sub>x</sub> Mask Layer

To clarify the super-RENS mechanism, the read/write characteristics are examined experimentally. The objective lens numerical aperture is NA = 0.5, the laser wavelength is  $\lambda = 826$  nm, providing the optical resolution limit  $\lambda/4NA = 413$  nm, and the disk velocity is  $v = 2$  m/s. To obtain the

maximum CNR of a reproduced signal, the disk is initialized at  $P_i = 3.5$  mW, at which completely decomposed Ag particles are dispersed in the mask layer.

#### 2.1 Write once performance

On the basis of the experimental comparison of the CNR and signal amplitude dependences on the writing power, the following read/write model of a super-RENS with a AgO<sub>x</sub> mask layer is clarified.<sup>4</sup> Both the mask and the recording layers have five possible states depending on the write power  $P_w$ : (a) as-deposited, (b) uniformly dispersed Ag particles (the diameter is estimated to be 8 nm)<sup>5</sup> and crystalline phase (after the initialization operation at  $P_i = 3.5$  mW), (c) Ag clusters and half amorphous phase ( $P_w = 4$ – $5$  mW), (d) Ag diffusion and completely amorphous phase ( $P_w = 5.5$ – $7.5$  mW), and (e) Ag rings and bubble pits (greater than  $P_w = 8$  mW). The mask layer for the super-resolution readout ( $P_r = 4$  mW) has a Ag ring structure, which increases both the CNR and resolution limit.

Because both the AgO<sub>x</sub><sup>6–8</sup> of the mask layer and the GST<sup>9–11</sup> of the recording layer are reversible at a laser power lower than that for deformation, a super-RENS disk with these layers is expected to be reversible if both layers are controlled independently using the appropriate laser powers and cooling rate.

#### 2.2 Rewrite performance

The CNR of a super-RENS disk with the mask layer made of AgO<sub>x</sub> and the recording layer made of GST varies not only with the phase change of the recording layer but also with that of the mask layer. We attempted to rewrite marks by changing write power, erase power, and superresolution read power, but it was unsuccessful. Therefore, we studied the reversible conditions for the mask layer in order to control the mask and recording layers independently. First, we found that as the number of initialization operation increases, the reflectivity varies in the beginning but saturates at a constant value, depending on the power, after 30 initialization operations, which is equivalent to a 5 s

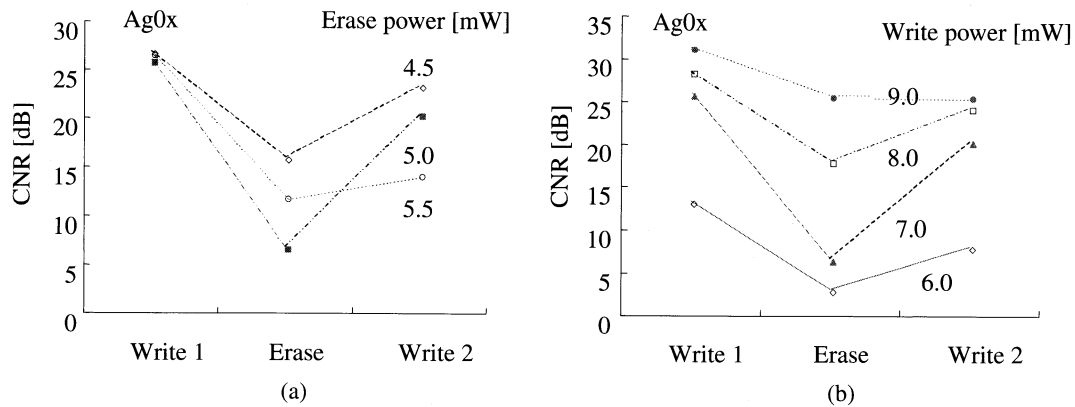


Fig. 1. Rewrite CNR for a mark length of 1000 nm at different erase powers with a write power of 7.0 mW (a), and rewrite CNR at different write powers with a erase power of 5.0 mW (b).

continuous initialization. Then we investigated the reversible condition for the initialized mask (5 s initialization at  $P_i = 4.5$  mW), and confirmed that a reversible change occurs after six illumination operations at  $P_i^1 = 2.5$  mW and one illumination operation at  $P_i^u = 3.5$  mW.

Figure 1(a) shows CNR for write 1 at  $P_w = 7.0$  mW, a superresolution read at  $P_{sr} = 4.0$  mW, 5 s erase at  $P_e$  mW, read at  $P_{sr} = 4.0$  mW, and write 2 (rewriting) for 1000-nm-mark trains, with the erase power  $P_e$  as a parameter. It is found that CNR decreases by 20 dB when erasing at  $P_e = 5.0$  mW and increases by 15 dB when rewriting at  $P_w = 7.0$  mW, resulting in a successful rewrite operation. Figure 1(b) shows CNR for write 1 at  $P_w$ , read at  $P_{sr} = 4.0$  mW, erase at  $P_e = 5.0$  mW for 5 s, read at  $P_{sr} = 4.0$  mW, and write 2 (rewriting) for 1000-nm-mark trains, with the write power  $P_w$  as a parameter. CNR varies most (15 dB) at  $P_w = 7.0$  mW but does not change at  $P_w = 9.0$  mW because of the deformation due to the high-power illumination.

On the basis of the results obtained above, a rewrite operation is possible for the AgO<sub>x</sub>-type super-RENS by performing the following steps.

1. Initialize the disk at  $P_i = 4.5$  mW for 5 s.
2. Write at  $P_w = 7.0$  mW.
3. Read at the superresolution power  $P_{sr} = 4.0$  mW.
4. Erase at  $P_e = 5.0$  mW for 5 s.
5. Read at  $P_{sr} = 4.0$  mW.
6. Rewrite at  $P_w = 7.0$  mW.

Finally, the rewrite operation is repeated as shown in Fig. 2, in which the difference in CNR between writing and erasing decreases as the number of rewrite operations increases, leading to four rewrite operations for the AgO<sub>x</sub>-type super-RENS.

### 3. Enhanced Rewrite Performance with a Ag<sub>2</sub>O Mask Layer

To improve the rewrite performance, the mask layer material is changed from AgO<sub>x</sub> to Ag<sub>2</sub>O.<sup>6)</sup> Because the reflectivity of Ag<sub>2</sub>O is higher than that of AgO<sub>x</sub>, more laser power is needed to change the phase of the mask layer and that of the recording layer, leading to similar laser powers needed for both layers. The configuration for the super-RENS optical disk with a Ag<sub>2</sub>O mask layer is PC substrate (0.6 mm)/ZnSiO<sub>2</sub> (130 nm)/Ag<sub>2</sub>O (20 nm)/ZnSiO<sub>2</sub> (40 nm)/GST (20 nm)/ZnSiO<sub>2</sub> (20 nm).

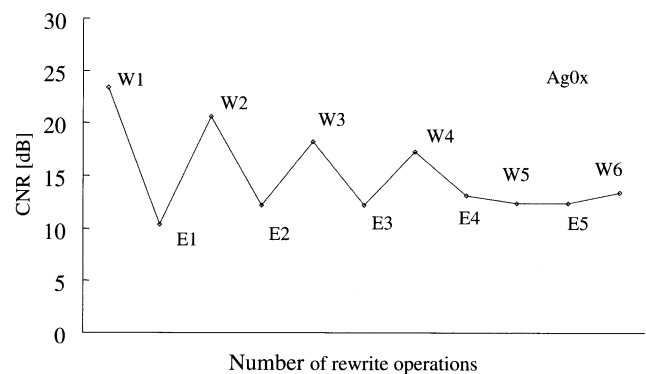


Fig. 2. CNRs of repeated 1000-nm-mark write and erase operations for the AgO<sub>x</sub>-type super-RENS optical disk.

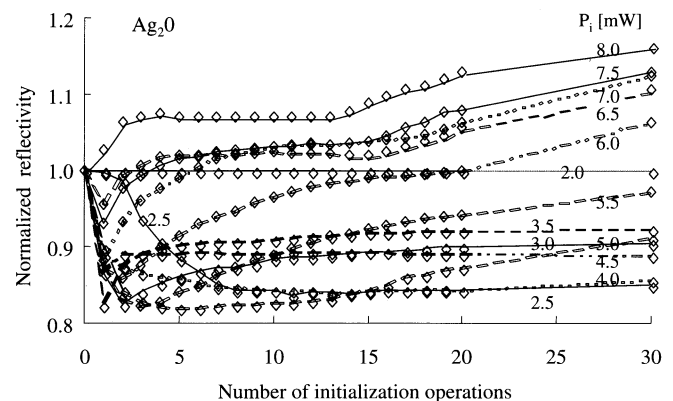


Fig. 3. Normalized reflectivity varying with the number of initialization operations for the Ag<sub>2</sub>O-type super-RENS optical disk, with initialization power as a parameter.

#### 3.1 Reversible conditions for the Ag<sub>2</sub>O mask layer

Figure 3 shows the relationship between reflectivity, normalized to as-deposited reflectivity, and the number of initialization operations with the power  $P_i$  as a parameter. At  $P_i = 2.5$  mW, reflectivity decreases to a saturation level owing to the initialization process of GST (recording layer) from the as-deposited amorphous phase to the fcc-structured crystalline phase ( $\alpha$  phase) as the initialization time increases, which is the same behavior as that in the digital versatile disk-random access memory (DVD-RAM) initial-

ization process (which usually requires 10 initialization operations). At  $P_i = 3.5$  mW, composite signals of the recording layer described above (which decreases reflectivity) and the mask layer ( $\text{Ag}_2\text{O}$  is decomposed into Ag nanoparticles, which increases reflectivity) appear because the decomposition temperature of  $\text{Ag}_2\text{O}$  and the initialization (first crystalline phase transition) temperature of GST are nearly the same about  $160^\circ\text{C}$ . This shows that the continuous illumination at 3.5 mW raises the temperature of a rotating disk to about  $160^\circ\text{C}$ , such that the illumination at 8.0 mW for writing described later will not cause the disk to reach the melting point of  $620^\circ\text{C}$ , but will cause it to reach the second-crystalline-phase-transition temperature range of  $250\text{--}450^\circ\text{C}$ .<sup>10</sup> The phase of the recording layer transforms from a rocksalt fcc structure ( $\alpha$  phase) to a hexagonal structure ( $\beta$  phase).<sup>11</sup>

At a large  $P_i$ , reflectivity decreases first, increases gradually, and then saturates at the 30th initialization, which means that  $\text{Ag}_2\text{O}$  is decomposed completely into Ag nanoparticles that aggregate to form nanoclusters, whose size depends on the power  $P_i$ , and that the Ag nanoclusters are dispersed in the mask layer. We used  $P_i = 8.0$  mW for the disk initialization because at this  $P_i$ , Ag nanoclusters are dispersed in the mask layer but no phase change occurs in the recording layer. Then we investigated the laser powers required for the reversible phase change of the mask layer, for which superresolution read power will be chosen to be between them, and observed the following, as shown in Fig. 4.

Figure 4 shows the normalized reflectivity for six illumination operations at  $P_i^1 = 4.5$  mW and one illumination operation at  $P_i^u = 6.0$  mW, with the number of initialization operations at the power  $P_i = 8.0$  mW as a parameter. Reflectivity increases and returns to 1.0 when a high power of  $P_i^u = 6.0$  mW is used for illumination but decreases when a low power of  $P_i^1 = 4.5$  mW is used for illumination and saturates to 0.94. Ag nanoparticles disappear by creating  $\text{Ag}_2\text{O}$  after six illumination operations at  $P_i^1 = 4.5$  mW, but Ag nanoparticles/nanoclusters appear by decomposing  $\text{Ag}_2\text{O}$  after one illumination operation at  $P_i^u = 6.0$  mW. The largest reflectivity variation occurs after 30 initialization operations at  $P_i = 8.0$  mW.

To confirm that this variation is irrelevant to the recording layer but depends on the reversible behavior of the mask layer, we write 1000-nm-mark trains at a write power  $P_w$  between 5.0 mW (less than  $P_i^u$ ) and 9.0 mW (upper limit

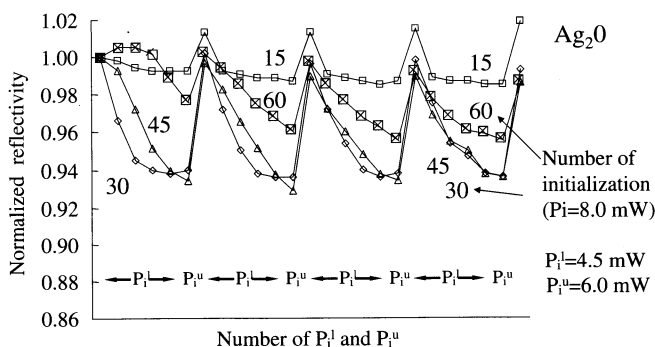


Fig. 4. Reversible characteristics of the mask layer realized using  $P_i^1 = 4.5$  mW and  $P_i^u = 6.0$  mW at  $P_i = 8.0$  mW with initialization number as a parameter.

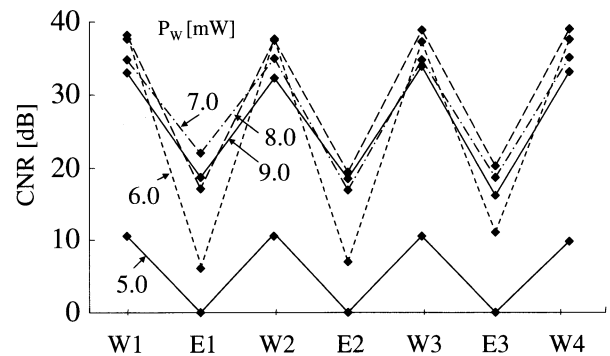


Fig. 5. CNR dependence on the write power  $P_w$  at 3 s erase power of  $P_e (= P_i^1) = 4.5$  mW.

of our experimental apparatus) after the continuous erase operation at the power  $P_e (= P_i^1) = 4.5$  mW. Figure 5 shows CNR, with the write power  $P_w$  as a parameter. It is found that the marks written at a pulsed power of  $P_w = 5$  mW are completely erased to 0 dB with continuous  $P_e (= P_i^1) = 4.5$  mW, but the marks written at  $P_w = 6$  mW are not completely erased, which suggests that the phase transition in the recording layer begins at the pulsed power  $P_w = 6$  mW. As a result, it is confirmed that the reversible change occurs in the mask layer that was initialized 30 times at  $P_i = 8.0$  mW. Thereafter, we use a continuous power of  $P_i = 8.0$  mW for 3 s, which corresponds to about 30 initialization operations in the experiment.

### 3.2 Rewrite signal quality (CNR)

Figure 6 shows the reproduced signals, with the read power of  $P_r = 1.0$  mW for 1000-nm-mark trains (a), and with the superresolution read power of  $P_{sr} = 5.5$  mW for 400-nm-mark trains (b). It is found that CNR reaches 42 dB (a), and the marks with a size less than the resolution limit  $\lambda/4\text{NA} = 413$  nm can be reproduced by the superresolution effect (b).<sup>4</sup> Figure 7 shows the relationship between the superresolution read CNR and the write power  $P_w$  for the mark lengths of 1000 and 600 nm. It is found that a peak appears at  $P_w = 6.0$  mW and a dip appears at  $P_w = 7.0$  mW for the 1000-nm-mark length. This behavior occurs owing to the combined signals from the mask and recording layers; namely, reflectivity increases owing to the  $\text{Ag}_2\text{O}$  decomposition to Ag particles in the mask layer, but it decreases due to the phase transition process, which begins at  $P_w = 6.0$  mW, in the recording layer.

To verify the rewrite capability, we attempted to perform write and erase operations at a write power  $P_w$  greater than 6.0 mW. Figure 8 shows the CNR for the 1000-nm marks, with the write power  $P_w$  and the erase power  $P_e$  as parameters. It is found that the difference in CNR between writing and erasing reaches 34 dB, the largest in the case of  $P_w = 8.0$  mW and  $P_e = 7.5$  mW, which improves the rewriting performance. Because the disk temperatures are expected to be almost the same at a pulsed power of  $P_w = 8.0$  mW and at a continuous power of  $P_e = 7.5$  mW, the crystalline fcc structure ( $\alpha$  phase) is generated by slow cooling at the continuous  $P_e = 7.5$  mW (erase), but the crystalline hexagonal structure ( $\beta$  phase) is generated by fast cooling at the pulsed  $P_w = 8.0$  mW (write).<sup>9</sup>

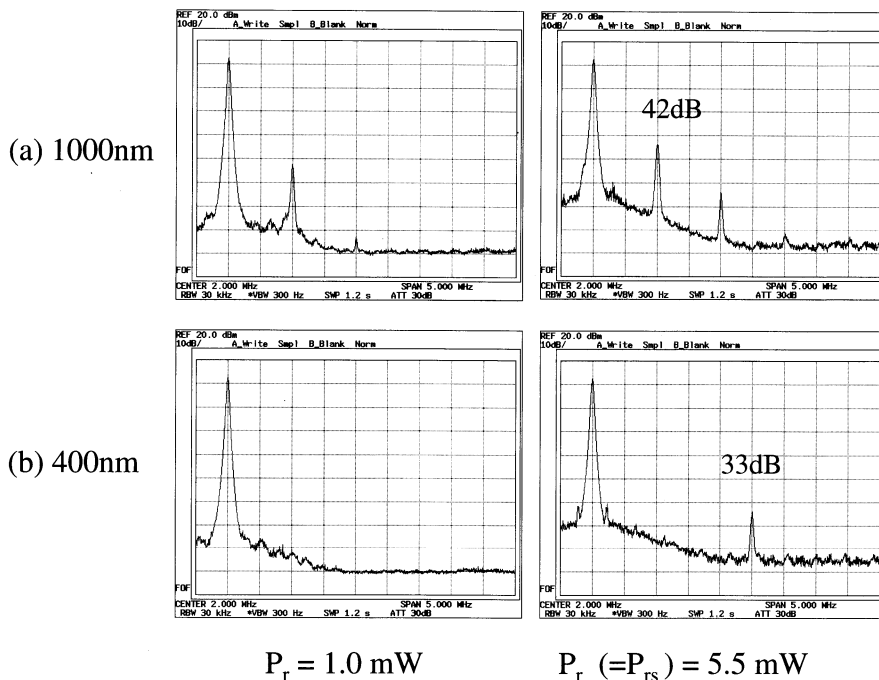


Fig. 6. Reproduced signals at a read power of  $P_r = 1.0$  mW for 1000-nm-mark trains (a), and at a superresolution read power of  $P_{sr} = 5.5$  mW for 400-nm-mark trains (b).

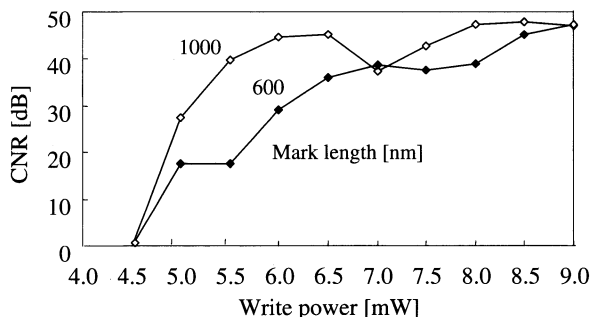


Fig. 7. Relationship between superresolution read CNR and write power  $P_w$  for mark lengths of 1000 and 600 nm.

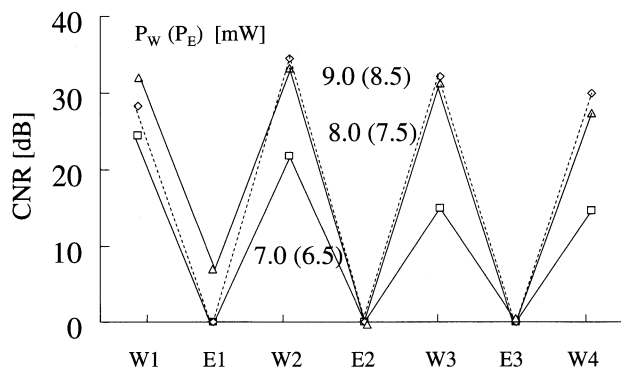


Fig. 8. CNR for the 1000-nm-mark train initialized using the 3 s  $P_i = 8.0$  mW, with the write power  $P_w$  and the erase power  $P_e$  as parameters.

Figure 9 shows the superresolution read signals for writing and erasing with different mark lengths: 500 nm (2 MHz), 400 nm (2.5 MHz), and 330 nm (3 MHz). It is found that the marks are completely erased to 0 dB for all mark lengths as shown in Fig. 10.

The results above suggest the following rewrite procedure for the  $Ag_2O$ -type super-RENS optical disk.

- (a) For the long-mark trains that can be read without the superresolution effect ( $P_r = 1.0$  mW).
  1. Initialize the disk at  $P_i = 8.0$  mW for 3 s.
  2. Write at a pulsed power of  $P_w = 8.0$  mW.
  3. Erase at  $P_e = 7.5$  mW for 3 s.
  4. Rewrite at a pulsed power of  $P_w = 8.0$  mW.
- (b) For the short-mark trains, whose length is less than the resolution limit  $\lambda/4NA$ , that are read with the super-resolution effect ( $P_{sr} = 5.5$  mW).
  1. Initialize the disk at  $P_i = 8.0$  mW for 3 s.
  2. Write at a pulsed power of  $P_w = 9.0$  mW.
  3. Read at the superresolution power of  $P_{sr} = 5.5$  mW (initialize the mask only).
  4. Erase at  $P_e = 7.5$  mW for 3 s.

5. Read at  $P_{sr} = 5.5$  mW (initialize the mask only).
6. Rewrite at a pulsed power of  $P_w = 9.0$  mW.

### 3.3 Number of rewrite operations

#### 3.3.1 Long marks (with lengths greater than the resolution limit $\lambda/4NA$ )

Figure 11 shows the repeated write and erase CNR reproduced at  $P_r = 1.0$  mW for a mark length of 1000 nm. The marks are written at a pulsed power of  $P_w = 8.0$  mW and are erased completely at  $P_e = 7.5$  mW for 3 s. CNR gradually decreases at first as the repetition number increases but saturates to 23 dB after 20 rewrite operations. The rewrite performance of the  $Ag_2O$ -type super-RENS is improved much compared with that of the  $AgO_x$ -type super-RENS as shown in Fig. 2.

#### 3.3.2 Short marks (with lengths less than the resolution limit $\lambda/4NA$ )

Figure 12 shows the repeated write and erase CNR reproduced at a superresolution power of  $P_{sr} = 5.5$  mW

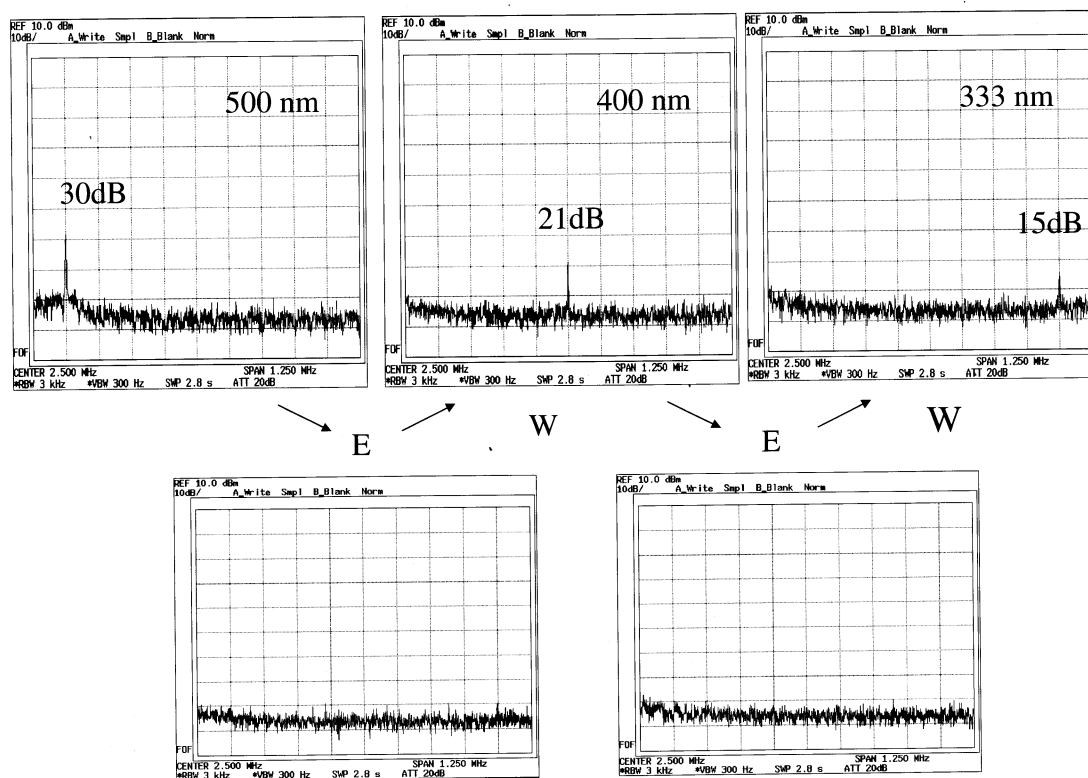


Fig. 9. Superresolution read signals for rewriting and erasing alternately with different mark lengths.

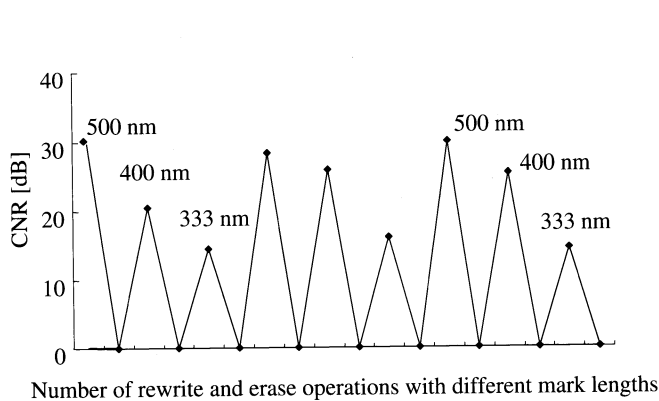


Fig. 10. CNR for rewriting at  $P_w = 9.0 \text{ mW}$  and erasing at  $P_e = 7.5 \text{ mW}$  alternately with different mark lengths.

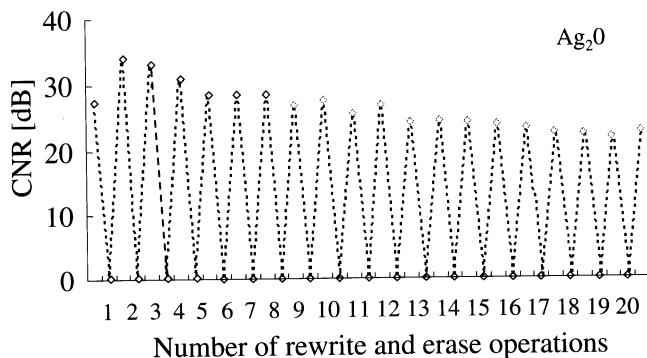


Fig. 11. CNR dependence on the number of operations of rewriting and erasing 1000-nm marks that can be read without superresolution readout ( $P_r = 1.0 \text{ mW}$ ) for the  $\text{Ag}_2\text{O}$ -type super-RENS disk.

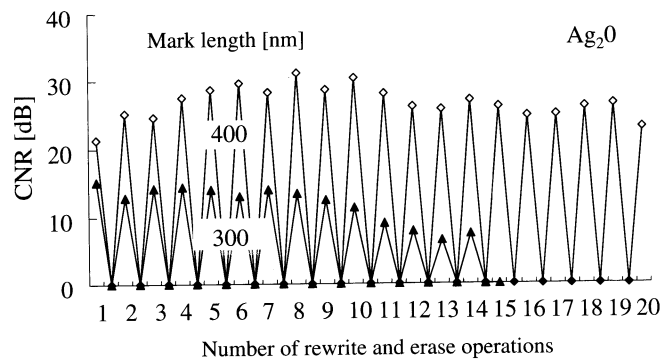


Fig. 12. CNR dependence on the number of rewrite operations with superresolution readout ( $P_{sr} = 5.5 \text{ mW}$ ) for the mark lengths of 400 and 300 nm, both of which are less than the resolution limit  $\lambda/4NA$ .

for mark lengths of 400 and 300 nm, both less than the resolution limit  $\lambda/4NA$  at a write power of  $P_w = 9.0 \text{ mW}$ . The marks are completely erased at  $P_e = 7.5 \text{ mW}$  after 3 s and the CNR for the 400 nm mark fluctuates but remains at 23 dB after 20 rewrite operations. On the other hand, the CNR for the 300 nm mark gradually decreases to 0 dB after 14 rewrite operations.

#### 4. Discussion on Rewriting Performance of the $\text{Ag}_2\text{O}$ -type Super-RENS

Figure 13 shows a summary of the experimental results for a disk velocity of 2 m/s, an objective lens numerical aperture of  $NA = 0.5$ , and a laser wavelength of  $\lambda = 826 \text{ nm}$  ( $\lambda/4NA = 413 \text{ nm}$ ). The upper row shows the phase of the mask layer, the middle row shows the laser powers needed to control the phase of the mask and recording layers, and the lower row shows the phase of the recording

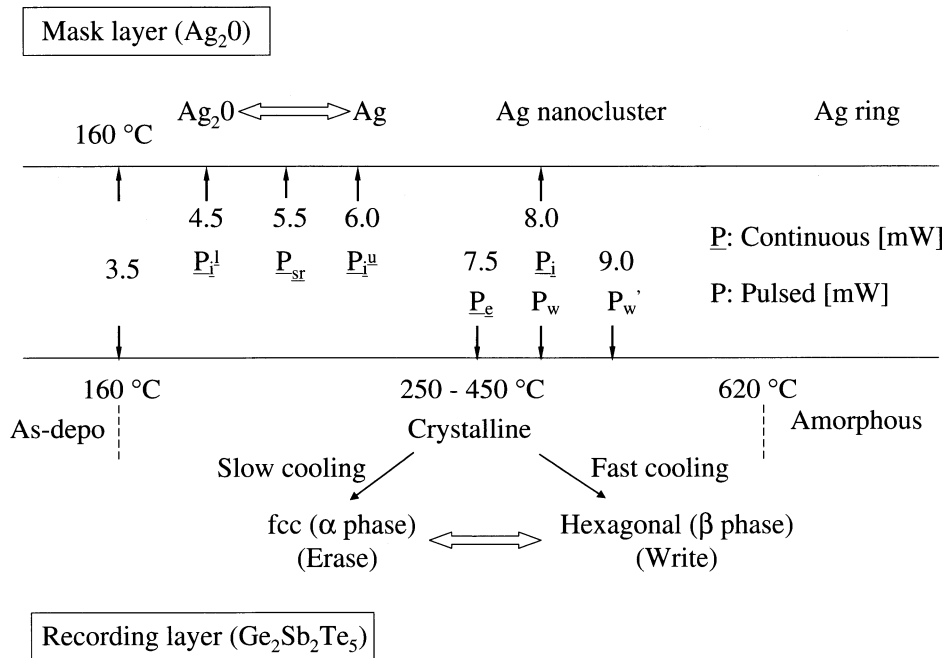


Fig. 13. Summary of the rewriting mechanism for the  $\text{Ag}_2\text{O}$ -type super-RENS optical disk obtained from systematic experiments for a disk velocity of 2 m/s, an objective lens numerical aperture of  $\text{NA} = 0.5$ , and a laser wavelength of  $\lambda = 826 \text{ nm}$  ( $\lambda/4\text{NA} = 413 \text{ nm}$ ).

layer. In the middle row,  $\underline{P}$  shows the continuous power that leads to slow cooling and  $\underline{P}$  shows the pulsed power that leads to fast cooling. We summarize the rewriting mechanism on the basis of the results shown in this figure.

For the initialization of the disk, 3 s of continuous  $P_1 = 8.0 \text{ mW}$  is needed, which leads to the dispersal of the aggregated Ag nanoclusters in the mask layer and the crystal  $\alpha$  phase in the recording layer owing to the slow cooling. After this initialization, the phase of the mask layer can be reversed by the six illumination operations at  $P_1^l = 4.5 \text{ mW}$  and by one illumination operation at  $P_1^u = 6.0 \text{ mW}$ . Normalized reflectivity increases to 1.0 when a high power of  $P_1^u = 6.0 \text{ mW}$  is used for an illumination but decreases when a low power of  $P_1^l = 4.5 \text{ mW}$  is used for illumination and saturates to 0.94. The superresolution read power of  $P_{sr} = 5.5 \text{ mW}$  is set between the two values.

To rewrite, we attempted to perform write and erase operations at a write power  $P_w$  greater than  $6.0 \text{ mW}$ , at which phase transition begins to occur in the recording layer. We found that the difference in CNR between writing and erasing reaches 34 dB, the largest in the case of  $P_w = 8.0 \text{ mW}$  and  $P_e = 7.5 \text{ mW}$  for a mark length of 1000 nm. Because the disk temperatures are expected to be almost the same at the pulsed  $P_w = 8.0 \text{ mW}$  and the 3 s  $P_e = 7.5 \text{ mW}$ , the crystalline  $\alpha$  phase (erase) is generated by the slow cooling at the continuous  $P_e = 7.5 \text{ mW}$ , but the crystalline  $\beta$  phase (write) is generated by the fast cooling at the pulsed  $P_w = 8.0 \text{ mW}$ .<sup>9)</sup> The second-phase-transition temperature range of crystalline is reported to be  $250 - 450^\circ\text{C}$ .<sup>10)</sup>

Because the operating laser powers for the  $\text{Ag}_2\text{O}$  mask layer ( $P_{sr} = 5.5 \text{ mW}$  and  $P_i = 8.0 \text{ mW}$ ) and those for the recording layer ( $P_e = 7.5 \text{ mW}$  and  $P_w = 8.0 - 9.0 \text{ mW}$ ) are close to each other, the mask layer is not degraded by the repeated write and erase operations, whereas degradation occurs for the  $\text{AgO}_x$  mask. A CNR of 25 dB after 20 rewrite operations was obtained for a mark length less than the

resolution limit  $\lambda/4\text{NA} = 413 \text{ nm}$ . To improve CNR, we need to not only optimize initialization power, erasing time, and other related parameters but also design the disk structure that includes protective layers.

## 5. Conclusions

To rewrite data on a double-layer optical disk such as the super-RENS disk, which contains a mask layer and a recording layer, we must control the layers independently. A rewritable mechanism for the  $\text{AgO}_x$ -type super-RENS disk is realized by introducing the mask layer initialization process before rewriting. Enhanced rewritable characteristics are obtained for the  $\text{Ag}_2\text{O}$ -type super-RENS disk by bringing the operating laser powers needed for the mask layer closer to those for the recording layer, thereby preventing the mask layer from being degraded by the successive rewrite and erase operations. The results obtained are summarized as follows for the enhanced super-RENS optical disk with the  $\text{ZnSiO}_2/\text{Ag}_2\text{O}/\text{ZnSiO}_2/\text{Ge}_2\text{Sb}_2\text{Te}_5/\text{ZnSiO}_2$  structure moving at a speed of 2 m/s:

- (1) Rewriting is realized for the disk initialized at  $P_i = 8.0 \text{ mW}$  for 3 s, resulting in Ag nanoclusters uniformly dispersed in the mask layer and a crystalline fcc structure ( $\alpha$  phase) in the recording layer.
- (2) The phase of the mask layer can be reversed from  $\text{Ag}_2\text{O}$  to Ag particles and *vice versa* using a power of  $P_1^l = 4.5 \text{ mW}$  (six illumination operations) and a power of  $P_1^u = 6.0 \text{ mW}$  (one illumination operation).
- (3) Rewriting is possible for the  $\text{Ge}_2\text{Sb}_2\text{Te}_5$  recording medium at a continuous erasing power of  $P_e = 7.5 \text{ mW}$  applied for 3 s and writing at a pulsed power of  $P_w = 8.0 - 9.0 \text{ mW}$ .
- (4) A CNR of 25 dB is realized after 20 rewrite operations for a mark length of 400 nm, which is less than the resolution limit ( $\lambda/4\text{NA} = 413 \text{ nm}$ ) of our experimental apparatus.

To further improve rewriting performance, the 3 s for initialization and erasing should be shortened, and the CNR should be increased to 50 dB.

### Acknowledgments

The authors would like to thank Dr. J. Tominaga of the National Institute of Advanced Industrial Science and Technology for discussion about the Ag<sub>2</sub>O and GST characteristics related to the super-RENS optical disk and Dr. T. Shima of the National Institute of Advanced Industrial Science and Technology for the preparation of the Ag-type super-RENS optical disks.

- 1) H. Fuji, J. Tominaga, L. Men, T. Nakano, H. Katayama, and N. Atoda: Jpn. J. Appl. Phys. **39** (2000) 980.
- 2) T. Kikukawa, A. Tachibana, H. Fuji, and J. Tominaga: Jpn. J. Appl. Phys. **42** (2003) 1038.
- 3) F. H. Ho, H. H. Chang, Y. H. Lin, B. M. Chen, S. Y. Wang, and D. P. Tsai: Jpn. J. Appl. Phys. **42** (2003) 1.
- 4) H. Ukita, Y. Ueda, and M. Sasaki: Jpn. J. Appl. Phys. **44** (2005) 197.
- 5) K. Kataja, J. Olkkonen, J. Aikio, and D. Howe: Jpn. J. Appl. Phys. **43** (2004) 160.
- 6) T. Fukaya, D. Buchel, S. Shinbori, J. Tominaga, and N. Atoda: J. Appl. Phys. **89** (2001) 6139.
- 7) X. Li, S. J. Kim, S. H. An, and S. Y. Kim: Jpn. J. Appl. Phys. **43** (2004) 5014.
- 8) Y. C. Her, Y. C. Lan, W. C. Hsu, and S. Y. Tsai: Jpn. J. Appl. Phys. **43** (2004) 7519.
- 9) N. Yamada, E. Ohno, K. Nishiuchi, N. Akahira, and M. Takao: J. Appl. Phys. **69** (1991) 2849.
- 10) J. Tominaga, T. Shima, M. Kuwahara, T. Fukaya, A. Kolobov, and T. Nakano: Nanotechnology **15** (2004) 411.
- 11) A. V. Kolobov, P. Fons, A. I. Frenkel, A. L. Ankudinov, J. Tominaga, and T. Uruga: Nat. Mater. **3** (2004) 703.